A New Actuator for On-Orbit Inspection

Benjamin Reinhardt† and Mason Peck

***Abstract*— Can you move along a surface in space without propellant or mechanical contact? This paper presents a new actuator, the induction coupler, which generates an eddy-current force between a robotic inspector and the conductive exterior of its target. This force allows the inspector to crawl along the surface of a target *without mechanical contact*. Sets of induction couplers composed of spinning arrays of permanent magnets can exert control force and torque in all six rigid-body degrees of freedom by strategically repelling and shearing across the surface of the target. This paper uses an analytical model of eddy-current forces to simulate the set of maneuvers necessary to produce the control force and torque that can move and orient a robotic orbital inspector. Experiments on a low-friction test bed demonstrate a successful implementation of the actuator and verify the feasibility of this approach.**

I. Introduction

On-orbit servicing (OOS) is a valuable but difficult robotic task[3][4][5]. Just as on earth, large assets like the International Space Station (ISS) or geostationary satellites experience wear and unexpected problems that require inspection, repair, or refuelling[7][13]. These tasks are well suited for robots because it is less dangerous and expensive to send an inspection vehicle to geostationary orbit or outside the ISS than a human spacewalker[1].

Maneuvering close to a target is essential to OOS and is a particularly risky proposition on orbit. On-orbit servicing requires a robotic spacecraft to operate in close proximity to the surface of a target in order to inspect, refuel, or repair it. Robotic operation in close proximity is difficult because spacecraft are fragile and respond to impacts with hard-to-predict rigid-body and flexible motions. There are presently three methods that permit an inspector to maneuver close to the surface of its target: it can mechanically grapple the surface to pull itself along; it can use propellant and thrusters; or it can use cooperative, non-contacting electromagnetic systems installed both on the inspector and the target. Grappling has many potential risks in an uncertain, low-friction environment[8]. Propellant is a finite resource and can damage sensitive surfaces through plume impingement[6]. Cooperation is infeasible in many situations because most spacecraft launch without the necessary subsystems: current spacecraft are *not* designed to be inspected or repaired by robots.

Fortunately, the ISS and most spacecraft are composed of aluminum plates, curves, and beams. New actuators can exploit that fact through eddy-current force. Specifically, by introducing a changing magnetic field, a robotic inspector can induce eddy currents in these non-magnetic but conductive components and use the reaction force between the field and the currents for actuation[14]. These eddy-current forces have several terrestrial applications from trash separation [12] to mag-lev propulsion,[11][9] but have never been used in robotics or orbital contexts. Induction couplers are actuators that utilize these eddy-currents. Their ability to actuate near a target with neither propellant nor mechanical contact can provide a completely new way to perform robotic locomotion and manipulation in space.

The first step towards an induction coupler locomotion system is to show how to produce actuation in each degree of freedom (DoF). What is it capable of given different states? Eddy-current forces depend both on the robot's pose and the geometry of the environment. Simulating a general eddy-current force is normally done with finite element analysis (FEA) [2]. However, FEA models are unsuitable for dynamic models of induction couplers for two reasons: time-domain simulation requires infeasibly long runtimes and the geometry would require re-meshing during the course of a simulation.

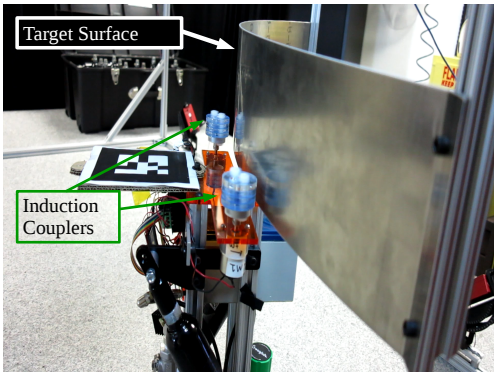

Fig. 1. An experimental inspector on a low-friction testbed uses induction couplers to actuate off of an aluminum plate simulating the ISS exterior.

Paudel and Bird derived an extensible analytical solution for eddy-current force near a flat plate that enables fast simulations of induction couplers[10]. This paper first extends the force model to include actuation force for arbitrary configurations of multiple induction couplers. The model leads to four basic control inputs and their associated motion primitives that can be combined to create six degree-of-freedom actuation: planar force (force in the plane of the target), planar torque (torque about an axis out of the plane), out-of-plane force, and out-of-plane torque. Each of these motions requires a different configuration of couplers and control input from those couplers. The objective of this

† B. Reinhardt and M. Peck are with the Department of Mechanical Engineering at Cornell University, 127 Upson Hall, Ithaca, NY 14850 bzr3@cornell.edu

paper is to demonstrate the basic capabilities of induction couplers and provide the motion primitives that can serve as the foundation for position controllers for robotic orbital inspectors.

Section II presents an analytical model to solve for induction-coupler force. Section III describes and simulates the open-loop behaviors that cause motion in each DoF. Finally, Section V presents experimental verification of each motion with a prototype induction coupler system on a low-friction testbed, shown in figure 1.

II. Actuator Model

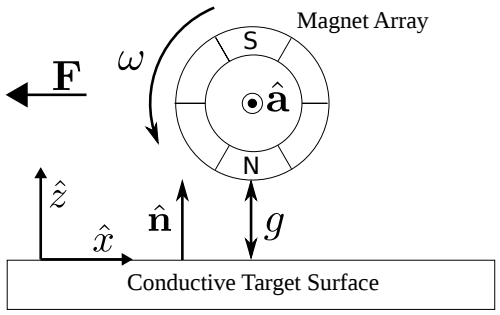

Fig. 2. Diagram of a single induction coupler array

Maxwell showed that a time-varying magnetic field induces an electric current in nearby conductors. Magnetic fields generate a force on moving currents. These two effects combine to create an eddy-current force between a source of a changing magnetic field and a conductive surface. Induction couplers can use mechanically moving permanent magnets or time-varying electromagnets to generate a time-varying magnetic field. This paper focuses on the simplest and least power-intensive implementation of a mechanical induction coupler: a motorized, circular array of magnets.

Paudel and Bird derived an analytical solution for the force from a single rotating array of permanent magnets near a flat conductor. [10] In a Newtonian reference frame fixed to the conductive surface shown in figure 2, the force on the magnet array is

$$ {}^{S}\mathbf{F} = \frac{w}{8\pi\mu_0}\int_{-\infty}^{\infty} \Gamma(\xi, g)|B^s(\xi, g)|^2 d\xi \tag{1} $$

where Γ is a transmission function associated with the conductive surface and B is the spatial Fourier transform of the time-invariant part of the array's magnetic field. Γ and B are nonlinear functions of the system state. Γ depends on the array's angular rate ω, velocity $\mathbf{v}$ and distance from the surface g. B is a nonlinear function of g as well. Near a curved surface of the scale of typical spacecraft, the assumption of an infinite flat surface is *locally* valid for induction couplers because the operating gap is on the order of centimeters: very small compared to the curvatures of most target surfaces.

Eddy-current properties and geometry can extend these forces from constrained, single wheel models to dynamic models of a 6-DoF orbital inspector. This extension is important because the coupler's axis is rarely perpendicular to the surface normal, and it is much more convenient to represent the forces in a global coordinate system instead of one fixed to the target surface. Eddy-current forces act only in opposition to change in magnetic field. So, the net force always acts in a direction perpendicular to the array's spin axis. Thus, a 3D formulation of the force in any reference frame can be found by tilting the force plane (shown in figure 2 along with $\hat{a}$.)

$$ \begin{aligned} \mathbf{F} =& F_z(g, \omega, \mathbf{v})\,(\hat{\mathbf{a}} \times \hat{\mathbf{n}}) \\ &+ F_y(g, \omega, \mathbf{v})\,(\hat{\mathbf{a}} \times \hat{\mathbf{n}}) \times \hat{\mathbf{a}} \end{aligned} \tag{2} $$

F_z and F_y are the components of the planar force calculated in equation 1.

This statement of eddy-current forces is powerful because it is both analytical and general. The generality enables fast simulations of a 6-DoF inspection vehicle while the analytical nature enables provable statements about the system's stability. A full system consists of several couplers to control all six DoFs. Each[M2] coupler rotates around an axis, $\hat{\mathbf{a}_n}$, located at $\mathbf{d}_n$, shown in figure 3. The net control force is

$$ \mathbf{F}_{net} = \sum_i F_z\,(\hat{\mathbf{a}}_i \times \hat{\mathbf{n}}_i) + F_y\,(\hat{\mathbf{a}}_i \times \hat{\mathbf{n}}_i) \times \hat{\mathbf{a}}_i \tag{3} $$

and the net control torque is

$$ \boldsymbol{\tau}_{net} = \sum_i \mathbf{d}_i \times [F_z\,(\hat{\mathbf{a}}_i \times \hat{\mathbf{n}}_i) + F_y\,(\hat{\mathbf{a}}_i \times \hat{\mathbf{n}}_i) \times \hat{\mathbf{a}}_i] \tag{4} $$

$\mathbf{n}_i$ is the vector to the surface segment closest to array i.

The following sections use this model to demonstrate how a robotic inspector can use induction couplers to generate force and torque in all six rigid body DoFs.

III. Movement Primitives

A. Planar Movement

While moving in the plane parallel to the target surface, induction couplers resemble contactless wheels, but they generate force parallel to the surface that increases with their speed. Thus, a fixed arrangement needs at least two couplers to move in all three planar DoFs and three couplers to control each DoF independently. Unlike wheels, induction couplers do not provide significant constraint force perpendicular to their rotation. They also cannot slip on the surface. So unlike wheels that skid if they accelerate too quickly, induction coupler forces are limited by the capabilities of their motors.

An inspector can translate in the plane by using a pair of induction couplers like differential drive wheels. Figure 3 shows this mode. Ideally, pure translational motion will involve no net torque. Applying these forces along a line of action that does not pass through the system's center of mass (CoM) naturally produces a torque. Without no-slip constraints, force and torque are coupled. Thus, the system is extremely sensitive to modeling error and implementing

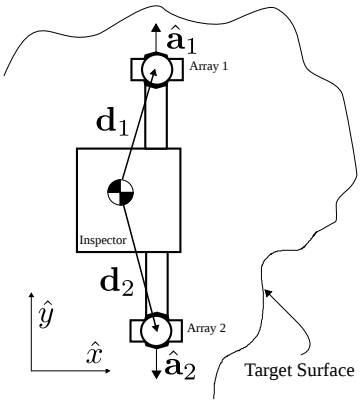

Fig. 3. Configuration for planar control: An inspector with two arrays spinning about $\hat{\mathbf{y}}$ can translate and rotate above a flat target surface

induction couplers for locomotion generally requires active control of all rigid-body DoFs.

An inspector also needs to rotate in the plane parallel to the surface. The simplest way for induction couplers to produce rotation about an axis normal to the surface without translation is similar to differential drive wheels, with two couplers spinning in opposite directions on axes parallel to the surface. Like pure translation, pure rotation in a real system is sensitive to the relative geometry of the coupler, the surface, and the CoM location, again demanding feedback control to decouple angular from translational motion.

B. Out-of-Plane Movement

It is more complicated for induction couplers to produce force and torque that control movement out of the plane parallel to the target surface because the forces from a single induction coupler are limited in their direction.

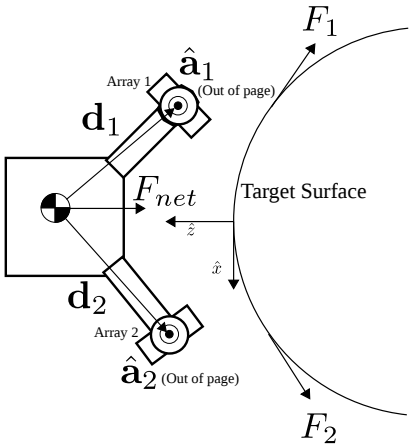

Fig. 4. Configuration for out-of-plane control

The force generated by spinning magnets is almost completely tangential to the surface. For large ω, the ratio of the normal to tangential components of the force increases slightly and can be used to repel away from the surface. However, these forces are small and act only in the $+\hat{\mathbf{z}}$ direction, giving no control in $-\hat{\mathbf{z}}$. By strategically summing forces across several couplers near different locations on a *non-flat* surface, the inspector can generate larger net forces in both $+\hat{\mathbf{z}}$ and $-\hat{\mathbf{z}}$.

Rotating two couplers oriented along the $\hat{\mathbf{y}}$ with opposing ω creates a force at each coupler whose $\hat{\mathbf{x}}$ components cancel and whose $\hat{\mathbf{z}}$ components sum, pulling the inspector towards the surface or pushing it away. This strategy is illustrated in figure 4.

Using tangential forces at each coupler, the inspector can control rotation about the $\hat{\mathbf{y}}$ axis by giving each coupler the same input speed ω. With only two couplers, force always couples with torque. A three-coupler array would allow the force and torque to be applied independently.

IV. Simulation

In this section, simulations demonstrate each motion primitive - planar translation, planar rotation, out-of-plane translation, and out-of-plane rotation. In each case, the simulation constrains the inspector to the plane of interest to demonstrate open-loop motion primitives - in practice, a closed loop controller and more than two couplers are essential to enable motion out of the plane. The model considers an inspector that is the size of a micro- or nanosatellite, using two motors each with two magnets as induction couplers. The model parameters shown in table I are those used in the experimental demonstrations in section V.

TABLE I
SIMULATION PARAMETERS

Description	value	units
Max Coupler Speed, ω	32.7	rad $s^{-}1$
Max Coupler Power, P_{max}	2	W
Max Magnet Shear Speed, v	0.98	$\frac{m}{s}$
Magnet Surface Field, B	4667	Gauss
Mass m	10.2	kg
Inertia $\mathbf{J}$	$1.02\mathbb{I}$	kgm^2
Gap in Planar Movement g	1	cm
Conductivity, σ	2.5×10^7	Sm^{-1}
Curvature of non-flat target, κ	0.14	m^{-1}

A. Planar Movement

To demonstrate planar movement, the target is represented by a flat conducting plate in the x-y plane shown in figure 3. In a simulation of planar translation the inspector first drives itself forward by commanding opposite speeds in each coupler. Because $\hat{\mathbf{a}}_1 = -\hat{\mathbf{a}}_2$, opposite speeds in the couplers result in both spinning in the same direction. The speeds of both couplers then reverse direction, creating a negative force and moving the inspector backwards. Figure 5 shows the coupler speeds, force, and displacement. In a simulation of planar rotation the inspector commands the same speed to each coupler, rotating itself about the positive z axis. The speeds of both couplers then reverse direction, generating a torque about the negative z axis. Figure 6 shows the coupler speeds, torque, and heading.

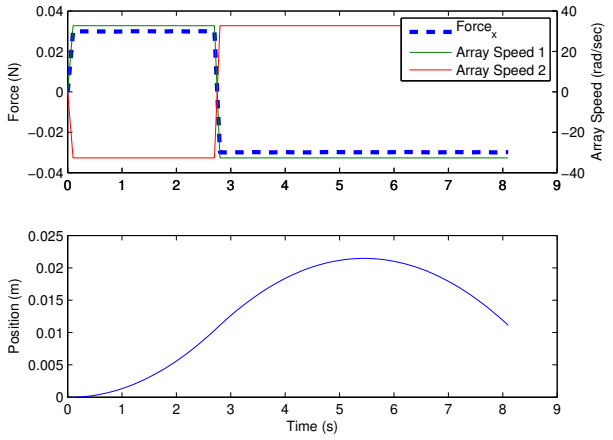

Fig. 5. Simulation of planar translation. The top plot shows the speed inputs to the couplers and resulting control force. The bottom plot shows the inspector's position

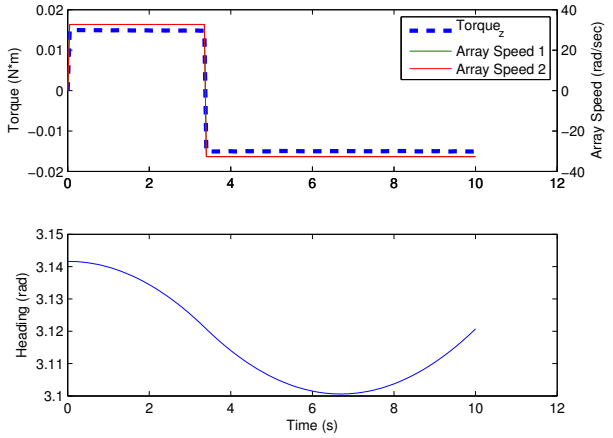

Fig. 6. Simulation of planar rotation. The top plot shows the speed inputs to the couplers and resulting control torque. The bottom plot shows the inspector's heading. Note: the control speed is the same for both arrays

B. Out-of-Plane Movement

To demonstrate out-of-plane movement, the target is a curved surface in the x-z plane, shown in figure 4. The surface curvature matches an ISS module both in simulation and experiment to approximate real capabilities as much as possible. The induction couplers both spin about the y axis in the body frame so that they can produce motion in the x-z plane by generating force tangential to the surface.

In figure 7 the inspector pulls itself towards the surface by spinning with opposing speeds so that the z component of each tangential force is negative. When the forces from each coupler sum, the resultant force is entirely in the -z direction, pulling the inspector towards the surface. The inspector then reverses the coupler speeds, pushing itself away from the surface and preventing a collision. Finally, it stops itself at its original position.

In figure 8 the inspector rotates about the y axis by spinning each coupler in the same direction.

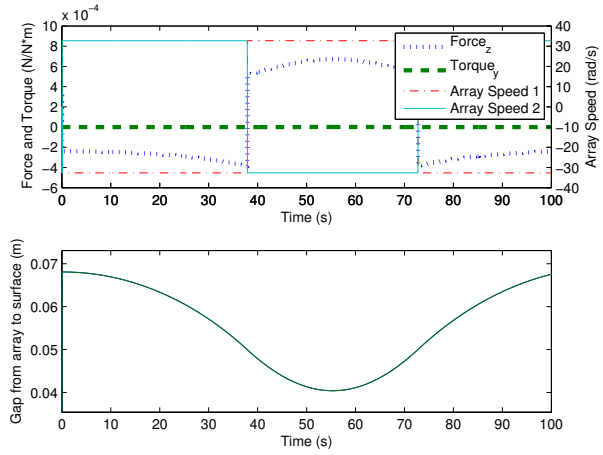

Fig. 7. Simulation of out-of-plane translation. The top figure shows the input speeds for each coupler and the resultant force on the inspector. The bottom figure shows how the gap between each coupler and the surface change in response to the control force

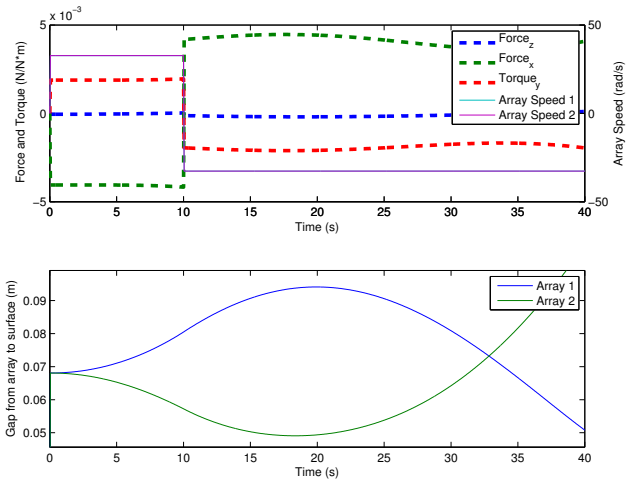

Fig. 8. Simulation of out-of-plane rotation. The top figure shows the input speeds for each coupler and the resultant force and torque on the inspector. The bottom figure shows how the gap between each coupler and the surface change in response to the control force and torque

V. Experimental Demonstration

This section discusses an experimental demonstration of each motion primitive–planar translation, planar rotation, out-of-plane translation, and out-of-plane rotation–in an ideal situation. The demonstration consists of two prototype inspection vehicles, each with two spinning magnet arrays. One prototype, pictured in figure 9, demonstrates the planar movement suggested in figure 3. The other prototype, pictured in figure 1, demonstrates the out-of-plane movement shown in figure 4. These inspection vehicle analogues operate on a low-friction air-bearing test bed, which allowed them to simulate a space-like environment with three DoFs.

The analogues operate close to, but not touching, an aluminum sheet-metal target during the experiments. During planar movement, a flat target sits above an analogue with arrays spinning about horizontal axes. Out-of-plane move-

ment uses a vertically oriented, curved target and vertical spin axes. The gap between the arrays and the target was approximately one centimeter (more precision is impossible because of imperfections in the arrays and the target.) A single experiment ended as soon as there was contact between an array and the surface or the gap between them grew large enough to neuter the actuator.

Hardware: The induction couplers are Sparkfun Standard DC Gearmotors, each with a laser-cut cylinder containing one north- and one south-facing neodymium magnet. A 12V lead-acid battery powers the motors. The properties of the magnets and motors are in table I. An Arduino microprocessor and Xbee radio enable remote open-loop commands and handle low-level motor control. A visual tag-based tracking system records the vehicle's heading and position with respect to the tags visible in figures 1 and 9. The aluminum target sits above the

Considerations: The arrays cannot be placed symmetrically about the center of mass due to the constraints of the test platform. Similarly, the tracking points cannot be located at the center of mass because the target occults it from the tracking system; the target plate was mounted directly above the vehicle out of necessity. These constraints mean that the experiments serve as a demonstration of individual motion primitives, rather than a full model validation.

A. Planar Movement

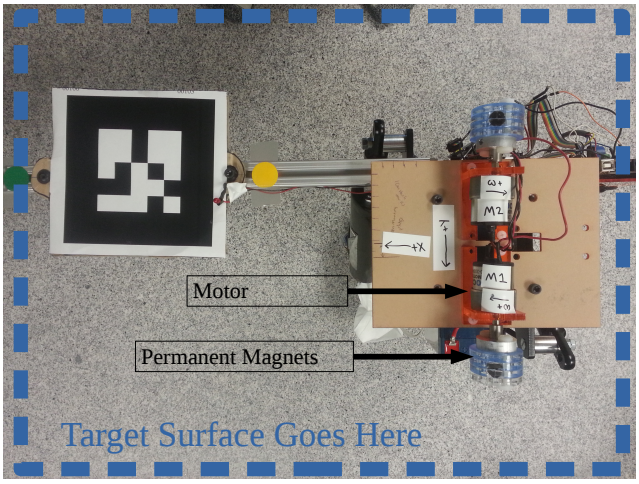

Fig. 9. Overhead view of the platform for demonstrating induction-coupler-generated planar motion

Figure 10 shows the trajectory of the inspector during planar translation. The inspector spins both arrays forward to translate forward. The majority of the inspector is obscured because the arrays needed to remain directly under the target surface.

Figure 11 shows a maneuver in which the inspector uses induction couplers to rotate itself around the $-\mathbf{z}$ axis and then reverses its motion by generating torque around $+\mathbf{z}$. Note that $\hat{\mathbf{a}}_1 = \hat{\mathbf{a}}_2$, the opposite of the simulations.

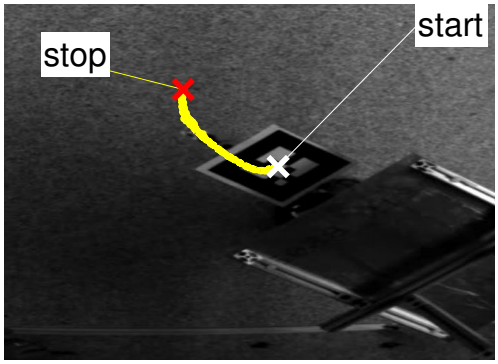

Fig. 10. Trajectory during a planar translation maneuver. The body of the inspector is obscured by the target surface in the lower right part of the picture

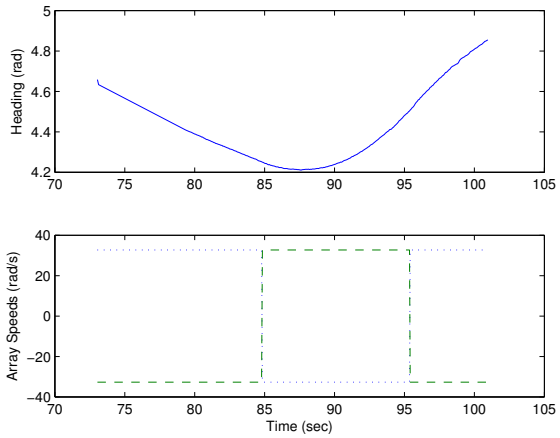

Fig. 11. Inspector heading (top) and induction coupler speed (bottom) during open-loop planar rotation

B. Out-of-Plane Movement

The plate used to demonstrate out-of-plane movement has a curvature designed to match the harmony module of the ISS. The inspector has two arrays, both with axes pointing in the $-\mathbf{y}$ direction, out of the page.

Figure 12 shows the results from the inspector pulling itself towards the surface. The distance it could travel before colliding with the plate is tiny, a clear motivation for closed-loop control. The bottom half of the figure shows the inspector accelerating towards the surface. The distance between the CoM and the plate decreases with an increasing rate.

Figure 13 shows the heading of the inspector as it rotates itself out of the plane about the $\hat{\mathbf{y}}$ axis.

VI. Conclusion

This paper focuses on modelling and demonstrating the ability of a system of induction couplers to actuate an orbital inspection vehicle in six DoFs near a conductive surface. Contactless, propellantless motion on orbit is unique capability that can form the basis of orbital servicing missions. The

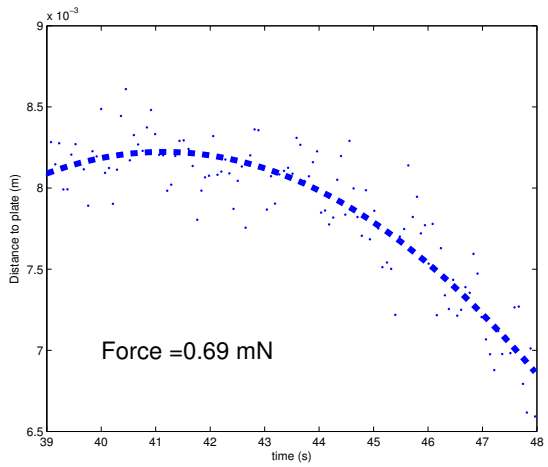

Fig. 12. Distance between plate and center of tag during out-of-plane translation. A quadratic fit indicates a constant force of 0.69 mN

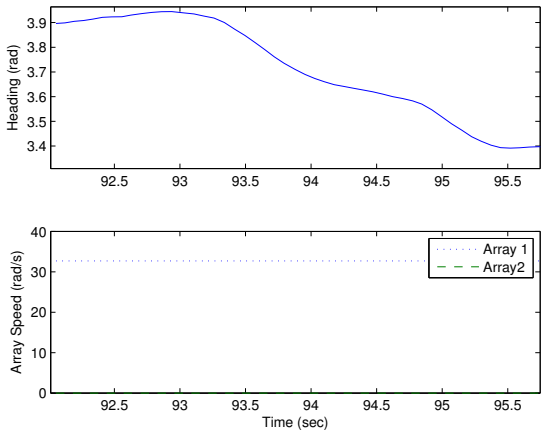

Fig. 13. Inspector heading (top) and coupler speeds (bottom) during out-of-plane rotation

construction of a generalized model enables fast dynamic simulations of an inspector using multiple induction couplers to actuate near a target surface. These couplers enable four different open-loop maneuvers that together span 6-DoF: planar translation, planar rotation, out-of-plane translation and out-of-plane rotation.

Theory and experiment show that couplers rotating on axes parallel to the plane generate planar motion similarly to a differential drive. Two or more couplers can take advantage of the surface geometry to generate motion out of the plane parallel to the target. This arrangement generates force in the $\hat{z}$ direction by two or more creating shear forces whose $\hat{x}$ and $\hat{y}$ components cancel but whose $\hat{s}$ components add. Flipping the direction of only one of these couplers produces a torque coupled with a force, enabling rotation out of the plane. Simulations demonstrate each of these four maneuvers in an ideal scenario and a prototype system on a low-friction air table shows that they work in practice as well as theory.

Future work will focus on two areas - adaptive controllers and movement planning. A robotic inspector will need adaptive controllers to account for induction coupler's strong dependence on poorly known parameters of the environment. The inspector will also need to plan movements carefully because its ability to exert control with an induction coupler is based on both its kinematics and the local geometry.

APPENDIX

The MATLAB code for simulating induction coupler actuated vehicles can be found at `https://github.com/bzreinhardt/induction_coupler_models`

ACKNOWLEDGMENT

This work was supported by NSTRF Grant #NNX11AN46H.
Thanks to the SPHERES team at NASA Ames for the test-bed and patient support.

REFERENCES

[1] Rob Ambrose, Brian Wilcox, Ben Reed, Larry Matthies, Dave Lavery, and Dave Korsmeyer. Robotics, Tele-Robotics and Autonomous Systems Roadmap. Technical report, NASA, 2012.

[2] Jonathan Bird and TA Lipo. Calculating the forces created by an electrodynamic wheel using a 2-D steady-state finite-element method. *Magnetics, IEEE Transactions on*, 44(3):365–372, 2008.

[3] E Coleshill, L Oshinowo, R Rembala, B Bina, D Rey, and S Sindelar. Dextre: Improving maintenance operations on the International Space Station. *Acta Astronautica*, 64(9-10):869–874, 2009.

[4] A Ellery. An engineering approach to the dynamic control of space robotic on-orbit servicers. *Proceedings of the Institution of Mechanical Engineers, Part G: Journal of Aerospace Engineering*, 218(2):79–98, 2004.

[5] A Ellery, J Kreisel, and B Sommer. Ellery, A, J Kreisel, and B Sommer. 2008. The Case for Robotic on-Orbit Servicing of Spacecraft: Spacecraft Reliability Is a Myth. Acta Astronautica 63 (5-6): 632648. doi:10.1016/j.actaastro.2008.01.042. ¡Go to ISI¿://WOS:000258632900010.The case for r. *Acta Astronautica*, 63(5-6):632–648, 2008.

[6] Gennady Markelov, Rolf Brand, Georg Ibler, and Wolfgang Supper. Numerical assessment of plume heat and mechanical loads and contamination on multi-layer insulation in hard vacuum. *Vacuum*, 86(7):889–894, 2012.

[7] S. Ali a. Moosavian and Evangelos Papadopoulos. Free-flying robots in space: an overview of dynamics modeling, planning and control. *Robotica*, 25(05):537–547, March 2007.

[8] Thai-Chau Nguyen-Huynh and Inna Sharf. Adaptive reactionless motion for space manipulator when capturing an unknown tumbling target. *2011 IEEE International Conference on Robotics and Automation*, pages 4202–4207, May 2011.

[9] Takahisa Ohji, Takashi Shinkai, Kenji Amei, and Masaaki Sakui. Application of Lorentz force to a magnetic levitation system for a non-magnetic thin plate. *Journal of Materials Processing Technology*, 181(1-3):40–43, January 2007.

[10] Nirmal Paudel and Jonathan Z. Bird. Modeling the Dynamic Electromechanical Suspension Behavior of an Electrodynamic Eddy Current Maglev Device. *Progress In Electromagnetics Research B*, 49(February):1–30, 2013.

[11] Nirmal Paudel and JZ Bird. General 2-D Steady-State Force and Power Equations for a Traveling Time-Varying Magnetic Source Above a Conductive Plate. *Magnetics, IEEE Transactions on*, 48(1):95–100, 2012.

[12] P C Rem and P A Leest. A model for eddy current separation. 16(96), 1997.

[13] J H Saleh, E Lamassoure, and D E Hastings. Space systems flexibility provided by on-orbit servicing: Part 1. *Journal of Spacecraft and Rockets*, 39(4):551–560, 2002.

[14] W.R Smyth. *Static & Dynamic Electricity*. 5th editio edition, 1989.